



## Article

# Pseudolite Multipath Estimation Adaptive Mitigation of Vector Tracking Based on Ref-MEDLL

Bo Zhang <sup>1</sup>, Qing Wang <sup>1,\*</sup>, Wenqing Xia <sup>1</sup>, Yu Sun <sup>2</sup> and Jinling Wang <sup>2</sup>

<sup>1</sup> School of Instrument Science and Engineering, Southeast University, No. 2 Sipailou Road, Nanjing 210096, China

<sup>2</sup> School of Civil and Environment Engineering, The University of New South Wales, Sydney 2052, Australia

\* Correspondence: wq\_seu@seu.edu.cn; Tel.: +86-025-8379-5562

**Abstract:** Among many indoor positioning technologies, pseudolite positioning technology has become an important supplement to GNSS. In indoor open environments, pseudolite positioning technology can usually perform high-precision positioning. However, in a complex environment, the pseudolite receiver is seriously interfered by multipath and other interference signals, which will lead to a serious decline in the observation accuracy, signal lock loss or even no positioning results. Therefore, this work proposes a pseudolite indoor anti-multipath receiver based on reference multipath estimating delay lock loop (Ref-MEDLL). It adds the Ref-MEDLL multipath estimator module and the multipath mitigation module to the traditional receiver signal processing architecture. In the multipath mitigation module, the multipath estimation adaptive mitigation of vector tracking (MEAM-VT) method and the multipath estimation direct mitigation (MEDM) method for multipath mitigation is proposed. Experimental results show that the Ref-MEDLL multipath estimation method has good adaptability to multipath signals that have different time delays and different amplitudes; both the MEDM receiver and the MEAM-VT receiver have good multipath mitigation performance. The MEAM-VT method performs better than the MEDM method in multipath mitigation and tracking, but the stability of the pseudorange observations of the MEAM-VT method is not as good as that of the MEDM method. The positioning accuracy of the MEDM receiver and the MEAM-VT receiver has been improved to different degrees in static positioning experiments and dynamic positioning experiments.

**Keywords:** pseudolite; indoor positioning; anti-multipath; Ref-MEDLL; multipath mitigation



**Citation:** Zhang, B.; Wang, Q.; Xia, W.; Sun, Y.; Wang, J. Pseudolite Multipath Estimation Adaptive Mitigation of Vector Tracking Based on Ref-MEDLL. *Remote Sens.* **2023**, *15*, 4041. <https://doi.org/10.3390/rs15164041>

Academic Editors: Giuseppe Casula and Baocheng Zhang

Received: 27 May 2023

Revised: 23 July 2023

Accepted: 13 August 2023

Published: 15 August 2023



**Copyright:** © 2023 by the authors. Licensee MDPI, Basel, Switzerland. This article is an open access article distributed under the terms and conditions of the Creative Commons Attribution (CC BY) license (<https://creativecommons.org/licenses/by/4.0/>).

## 1. Introduction

A pseudolite system can be used for indoor positioning as it can be deployed in indoor environments. Due to the unique complex environment and a large number of walls indoors, the indoor multipath effect will be more serious than the outdoor multipath effect. In indoor environment, the multipath effect will not only decrease positioning accuracy, but also may cause the direct loss of lock of the tracked signal in the receiver [1]. Indoor multipath can cause a positioning error in tens of meters, which seriously affects indoor positioning services [2]. Therefore, anti-multipath methods in complex indoor environments are indispensable for pseudolite receivers [3].

Since the pseudolite system is similar to GNSS, the anti-multipath method used by GNSS receivers is also applicable to pseudolite receivers. In fact, the multipath mitigation requirements for indoor pseudolite receivers are higher than those for GNSS receivers. Therefore, the pseudolite receivers should enhance their anti-multipath strategies, especially for indoor environment with complex conditions. The anti-multipath algorithm based on data processing has gained significant attention in recent years. Its core emphasis is on multipath parameter estimation [4,5]. Currently, several multipath estimation algorithms are prevalent, including extended Kalman filter (EKF) [6–8], particle filter (PF) [9,10],

maximum-likelihood estimation (MLE) [11], etc. Among many multipath estimation techniques, the most typical one is the technique based on MLE. The multipath estimating delay lock loop (MEDLL) [12,13] is the earliest MLE technology proposed. At present, there are a large number of improved methods based on MEDLL. Townsend et al. [14] review the multipath problem in the GPS receiver and the theory of the MEDLL. Brodin et al. [15] describe the analysis that has been carried out into code and carrier tracking in the presence of multipath. Fernández et al. [16] study performance analysis and parameter optimization of DLL and MEDLL in fading multipath environments for next generation navigation receivers. Tamazin et al. [17] introduce a robust multipath mitigation technique based on fast orthogonal search to obtain better delay estimation for GPS receivers. The PF are widely used to solve non-linear filtering problems without limitation of Gaussian distribution, and GNSS multipath estimation and mitigation based on particle filter are proposed [18]. The multipath estimating delay lock loop (MEDLL), which is originally designed for global positioning system receivers, is applied to LTE signal TOA estimation in multipath environments [19]. In indoor environments, it is common for pseudolite multipath signals to exist in multiple paths due to obstructions or reflections from various objects, such as walls, pillars, and furniture [20]. However, previous research on enhancing multipath estimation algorithms has predominantly assumed the presence of a single multipath signal or concentrated on improving each individual path independently, despite considering multiple multipath signals in the model.

Indeed, there have been algorithms proposed to estimate or calculate the number of multipath signals. One algorithm is the TK-MEDLL algorithm [21], which utilizes the TK (Teager–Kaiser) operator [22] to determine the number of multipath signals and their approximate delays. Subsequently, MEDLL is employed to achieve precise parameter estimation. The algorithm has been demonstrated to be effective in outdoor environments based on measured data. However, it is important to note that these algorithms may still have limitations or room for further improvement [23]. It is true that the sensitivity of the TK operator to noise increases as the correlator's resolution improves, creating a dilemma between estimation accuracy and noise sensitivity. This trade-off needs to be carefully considered when using the TK-MEDLL algorithm. Additionally, the grid MEDLL algorithm is another approach that can be used for multipath number estimation [24,25]. The grid MEDLL algorithm follows an initial assumption that assigns a specific delay value to each multipath signal, and then determines the existence of a multipath signal based on the obtained amplitude. However, this method, similar to TK-MEDLL, faces challenges in achieving a proper balance between estimation accuracy and noise sensitivity. A large preliminary study was carried out regarding the multipath signal estimation in the early stage [26]. This study builds upon the in-depth research conducted in previous published work and explores a new theory that utilizes reference MEDLL (Ref-MEDLL) multipath estimation results for multipath mitigation.

This study introduces a Ref-MEDLL multipath estimator module and two types of multipath suppression modules into the conventional receiver signal processing architecture, with the objective of achieving real-time multipath suppression. First, a Ref-MEDLL estimator is incorporated into the receiver to estimate the parameters of the multipath signal. Subsequently, two anti-multipath methods based on the Ref-MEDLL estimator are proposed, namely, multipath estimation direct mitigation (MEDM) and multipath estimation adaptive mitigation of vector tracking (MEAM-VT). The MEDM method utilizes the multipath parameter estimates obtained from the Ref-MEDLL estimator to directly eliminate multipath interference from the correlation curve. The MEAM-VT method incorporates the estimated multipath parameter results into the navigation filter of the vector tracking receiver, aiming to achieve real-time multipath mitigation. Vector tracking (VT) is a receiver technology that utilizes vector signal processing to improve the vector delay lock loop (VDLL) of multi-channel signals [27–29]. It employs advanced digital signal processing algorithms to directly process the received pseudolite signals in their complex form, which includes both the amplitude and phase information, rather than extracting

only the amplitude information. The indoor multipath signals from pseudolites can be decomposed into complex vector forms of line-of-sight (LOS) signals and non-line-of-sight (NLOS) signals, which can be processed in a VT receiver [30]. Ref-MEDLL multipath estimation parameters can help in improving the vector tracking loop in pseudolite receivers. The experimental results of this study demonstrate that the Ref-MEDLL module is capable of accurately estimating the parameters of multipath signals. Furthermore, both the MEDM method and the MEAM-VT method exhibit effective suppression of multipath signals.

In the following sections, the Ref-MEDLL multipath estimation theory and multipath mitigation methods are presented in Section 2. The experimental test and performance analysis of the multipath estimation and multipath mitigation algorithm are carried out in Section 3. Then, the advantages and limitations of the above multipath mitigation algorithm and the ideas for the improvement of this algorithm in the future are discussed in Section 4. Conclusions are presented in Section 5.

## 2. Materials and Methods

### 2.1. Multipath Signal Model

The signal received in a pseudolite receiver can typically be expressed as [31]:

$$s(t) = \sum_{i=0}^M s_i(t) + wn(t) = \sum_{i=0}^M \alpha_i c(t - \tau_i) e^{j(\omega t + \varphi_i)} + wn(t), \quad (1)$$

where  $s_i(t)$  represents the signal of  $i$ th path;  $\alpha_i$ ,  $\tau_i$ ,  $\varphi_i$  represent the amplitude, the delay relative to the local C/A code, and the phase relative to the local carrier of the  $i$ th path's signal;  $c(t)$  represents C/A code (navigation messages are ignored);  $wn(t)$  represents environmental noise;  $i = 0$  indicates that the signal is a LOS signal;  $M$  indicates the number of multipath signals; and  $\omega$  stands for carrier frequency.

The received IF signal is initially multiplied and mixed with the local carrier. It is then subjected to a low-pass filter to eliminate the high-frequency components. Finally, the resulting signal is correlated with the local C/A code. Assuming that the delay of the  $k$ th correlator is  $\tau_k$ , the correlation result can be expressed as:

$$R_k = R_x(\tau_k) = \sum_{i=0}^M \alpha_i R(\tau_k - \tau_i) e^{j\varphi_i} + n(\tau_k), \quad (2)$$

where  $R_k$  represents the result of the  $k$ th correlator;  $R_x(\tau)$  represents the correlation curve composed of all the results;  $R(\tau)$  represents the autocorrelation function of C/A code; and  $n(\tau)$  is the environmental noise after frequency mixing correlation.

Based on the principle of maximum-likelihood estimation, the Ref-MEDLL algorithm estimates the multipath parameters  $\alpha_i$ ,  $\tau_i$ , and  $\varphi_i$  of each multipath signal with the correlation curve  $R_x(\tau)$ , and then mitigates them.

### 2.2. Anti-Multipath Receiver Signal Processing Flow Architecture

In the pseudolite signal receiver, the basic steps of signal processing include acquisition, tracking, and PVT module [32]. The multipath signal mitigation problem mentioned in this paper is mainly realized by improving the receiver tracking module. Therefore, an anti-multipath receiver was designed, which added the Ref-MEDLL multipath estimation module and the multipath mitigation module to the tracking loop of the traditional receiver. As shown in Figure 1, the Ref-MEDLL multipath estimation module is used to estimate the number and parameters of multipath signals. Then, the multipath mitigation module eliminates the interference of the multipath signal and reconstructs the correlation curve  $R(\tau)$ . The innovative part of this work is the multipath mitigation module based on Ref-MEDLL. Two multipath signal mitigation methods have been proposed: the MEDM and the MEAM-VT. With the help of multipath mitigation module, the receiver eliminates the influence of multipath signals, which improves the accuracy of navigation and positioning.

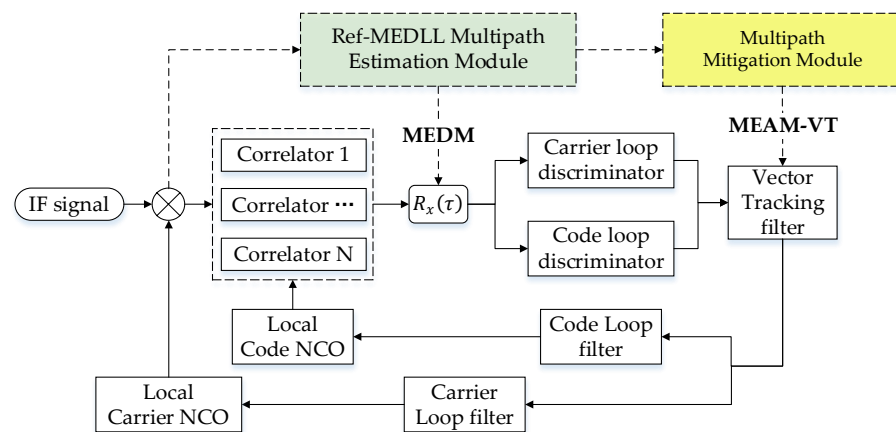


Figure 1. Signal processing structure diagram of Ref-MEDLL receiver.

The correlation result  $R_x(\tau)$  is obtained by performing the correlation operation on the signal with multiple correlators. After Ref-MEDLL’s multipath estimation of  $R_x(\tau)$ , the estimation results of parameters  $\hat{\alpha}_i$ ,  $\hat{\tau}_i$ , and  $\hat{\phi}_i$  of each multipath signal can be obtained, and their corresponding correlation curve can be calculated according to these parameters:

$$\hat{R}_i(\tau) = \hat{\alpha}_i R(\tau - \hat{\tau}_i) e^{j\hat{\phi}_i}. \tag{3}$$

Then, the estimated value of the noise correlation result  $R'_k$  can be estimated by subtracting the correlation curves corresponding to all multipath signals from the original correlation results, which means:

$$R'_k = R'_x(\tau_k) = R_x(\tau_k) - \sum_{i=0}^M \hat{R}_i(\tau) = R_x(\tau_k) - \sum_{i=0}^M \hat{\alpha}_i R(\tau_k - \hat{\tau}_i) e^{j\hat{\phi}_i} = \hat{n}(\tau_k). \tag{4}$$

At the same time, by choosing an appropriate time delay  $\tau_{ref}$ , the result of the reference correlator can be made to be the measurement of the noise correlation result  $R_{ref} = n(\tau_{ref})$ .

By comparing  $R'_k(t)$  and  $R_{ref}(t)$  with the multipath signal number estimation strategy, the number of multipath signals can be obtained gradually and used to correct the Ref-MEDLL multipath estimation.

### 2.3. Ref-MEDLL Multipath Signal Estimation

Ref-MEDLL is an enhancement of the previous adaptive-MEDLL approach [26]. The Ref-MEDLL multipath signal estimator operates by decomposing each multipath signal into N signal vectors, each with a distinct time delay. Estimating the number of multipath signals entails estimating the number of signal vectors, while the estimation of multipath signal parameters involves estimating the amplitude, time delay, and phase parameters of the signal vector. Ref-MEDLL enhances the multipath number estimator and strengthens the verification link of the multipath number estimation result. This refinement leads to more accurate multipath estimation numbers, resulting in reduced error rates and missed detection rates during multipath signal detection. Accurate estimation of multipath parameters, such as multipath amplitude, time delay, and phase, forms the basis for multipath parameter estimation. The multipath estimation process uses multiple correlators to improve the resolution of the multipath estimation, but this consumes a large amount of computing power. The results of the reference correlator proposed in this paper use the correlation results of real-time data as a reference, but empirical values can be used in the future. The method of deep learning will be used to train the correlation values of a large number of pseudolites in indoor complex environments to ensure the accuracy of reference values.

### 2.3.1. Multipath Signal Parameter Estimation

The multipath parameter estimation process of Ref-MEDLL is similar to that of traditional MEDLL algorithm [33,34]. When the number of multipath signals  $M$  is known, the multipath estimation process used by Ref-MEDLL algorithm and traditional MEDLL algorithm starts from the first signal. The estimation parameters are continuously optimized in cycle as the number of signals increases until the number of signals reaches  $M + 1$ . The flowchart of the Ref-MEDLL algorithm is shown in Figure 2:

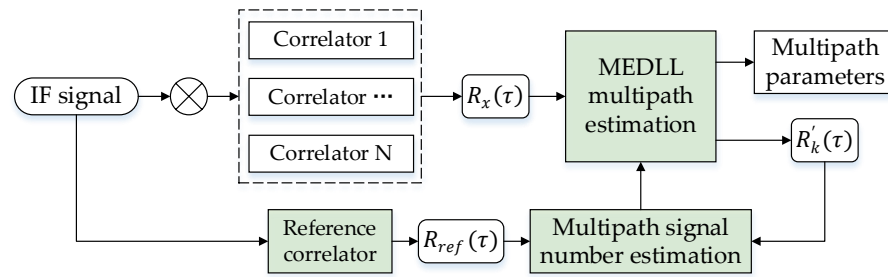


Figure 2. Ref-MEDLL algorithm flowchart.

Given the correlation function  $R_i(\tau)$ , the steps to calculate its signal parameters and generate the reconstruction correlation function are given as follows:

- (1) Phase estimation  $\hat{\phi}_i$

Find the delay corresponding to the maximum power sampling value in  $R_i(\tau)$ :

$$\tau_{\max} = \max_{\tau} \left\{ [\text{Re}(R_i(\tau))]^2 + [\text{Im}(R_i(\tau))]^2 \right\}, \tag{5}$$

where Re means Real, and Im means Imaginary. Then, the phase estimation result  $\hat{\phi}_i$  is obtained by the arctangent method:

$$\begin{aligned} \text{If } \text{Re}[R_i(\tau_{\max})] > 0, \quad \text{Then } \hat{\phi}_i &= \arctan \left\{ \frac{\text{Im}[R_i(\tau_{\max})]}{\text{Re}[R_i(\tau_{\max})]} \right\} \\ \text{If } \text{Re}[R_i(\tau_{\max})] < 0, \quad \text{Then } \hat{\phi}_i &= \arctan \left\{ \frac{\text{Im}[R_i(\tau_{\max})]}{\text{Re}[R_i(\tau_{\max})]} \right\} + \pi \\ \text{If } \text{Re}[R_i(\tau_{\max})] = 0 \ \& \ \text{Im}[R_i(\tau_{\max})] > 0, \quad \text{Then } \hat{\phi}_i &= \frac{\pi}{2} \\ \text{If } \text{Re}[R_i(\tau_{\max})] = 0 \ \& \ \text{Im}[R_i(\tau_{\max})] < 0, \quad \text{Then } \hat{\phi}_i &= -\frac{\pi}{2} \end{aligned} \tag{6}$$

Using the obtained phase estimation  $\hat{\phi}_i$ , the phase information in the correlation function can be removed, in order that the energy is concentrated in I channel, and the correlation function of the real number  $RI_i(\tau)$  can be obtained:

$$RI_i(\tau) = \text{Re}[R_i(\tau)] \cdot \cos(\hat{\phi}_i) + \text{Im}[R_i(\tau)] \cdot \sin(\hat{\phi}_i). \tag{7}$$

Then, the real correlation function can be used to estimate the delay  $\hat{\tau}_i$  and amplitude  $\hat{a}_i$ .

- (2) Delay estimation  $\hat{\tau}_i$

The phase discriminating function method is used to estimate the delay. A sampling point is selected as the correlation point of prompt code, and the correlation interval is selected for phase discrimination. According to the phase detection result, the difference between the actual delay and the correlation point of the prompt code is obtained, and then the actual delay is obtained. This paper is proposed to use Strobe correlator for delay estimation, and the specific steps are as follows:

Step 1: Before starting signal processing, the phase discrimination function  $e = D(\varepsilon)$  and its inverse function  $\varepsilon = D^{-1}(e)$  of phase detector should be calculated in advance.

Step 2: Select sampling point  $\tau_x$ . In order to reduce the influence of noise, and to ensure the monotonicity of the actual function of phase discrimination, the point  $\tau_{max}$  with the maximum power should be selected.

Step 3: Phase identification. First, the correlation interval  $\Delta\tau$  is determined, and then the five-way EPL correlation (Early-Prompt-Late:  $P, E_1, E_2, L_1, L_2$ ) results are obtained:

$$\begin{aligned} P &= RI_i(\tau_x) \\ E_1 &= RI_i\left(\tau_x - \frac{1}{2}\Delta\tau\right) \\ L_1 &= RI_i\left(\tau_x + \frac{1}{2}\Delta\tau\right), \\ E_2 &= RI_i(\tau_x - \Delta\tau) \\ L_2 &= RI_i(\tau_x + \Delta\tau) \end{aligned} \quad (8)$$

Then, they are placed into the phase detector to achieve the phase detection result:

$$e_x = \frac{2(E_1 - L_1) - (E_2 - L_2)}{P}. \quad (9)$$

Step 4: Obtain the bias. The deviation  $\varepsilon_x = D^{-1}(e_x)$  can be obtained by substituting  $e_x$  into the inverse function of the phase discriminator function. Since the value of the function calculated beforehand is discrete, if the obtained  $e_x$  is not among them, the linear difference method can be used to obtain the approximation. When  $e_1 \leq e_x \leq e_2$ , then:

$$\varepsilon_x = D^{-1}(e_1) + \frac{D^{-1}(e_2) - D^{-1}(e_1)}{e_2 - e_1}(e_x - e_1). \quad (10)$$

Step 5: Obtain the result. Theoretically,  $\varepsilon_x$  should not be greater than  $\frac{\Delta\tau}{2}$ . If  $\varepsilon_x \leq \frac{\Delta\tau}{2}$ , then the phase detector works normally, and the estimation result of delay  $\tau_i$  is  $\hat{\tau}_i = \tau_x - \varepsilon_x$ . However, if  $\varepsilon_x > \frac{\Delta\tau}{2}$ , then the phase detector does not work normally, which may be caused by excessive noise or multipath interference. The phase detection result should be discarded, then  $\hat{\tau}_i = \tau_x$ .

### (3) Amplitude estimation $\hat{\alpha}_i$

If  $\varepsilon_x \leq \frac{\Delta\tau}{2}$ , then the phase detector is working properly and it can be assumed that the proportion of  $RI_i(\tau)$  is the same as the reference correlation function  $R(\tau)$  in this range:

$$\frac{R(0)}{R(\varepsilon_x)} = \frac{RI_i(\tau_i)}{RI_i(\tau_i + \varepsilon_x)} = \frac{RI_i(\tau_i)}{RI_i(\tau_x)} = \frac{\alpha_i}{RI_i(\tau_x)}, \quad (11)$$

which means the amplitude estimation  $\hat{\alpha}_i$  is:

$$\hat{\alpha}_i = \frac{R(0)}{R(\varepsilon_x)} RI_i(\tau_x). \quad (12)$$

Otherwise, if  $\varepsilon_x > \frac{\Delta\tau}{2}$ , then:

$$\hat{\alpha}_i = RI_i(\tau_x). \quad (13)$$

### (4) Reconstruction correlation function generation

After the phase estimation  $\hat{\phi}_i$ , delay estimation  $\hat{\tau}_i$ , and amplitude estimation  $\hat{\alpha}_i$  are all completed, the correlation function can be reconstructed. Its value is:

$$\hat{R}_i(\tau) = \hat{\alpha}_i R(\tau - \hat{\tau}_i) e^{j\hat{\phi}_i}. \quad (14)$$

### 2.3.2. Multipath Signal Number Estimation

From the MEDLL Multipath Estimation process, we can see that this algorithm requires the number of multipath signals to be specified. Therefore, this paper proposes an algorithm to estimate the multipath signal number in indoor environment.

As mentioned above, after MEDLL multipath estimation of  $R_x(\tau)$ , the estimation results of parameters  $\hat{\alpha}_i$ ,  $\hat{\tau}_i$ , and  $\hat{\phi}_i$  of each multipath signal can be obtained, and their corresponding correlation curve  $\hat{R}_i(\tau)$  can be calculated according to these parameters. The estimated value of the noise correlation result  $R'_k$  can be obtained by subtracting the correlation curves corresponding to all multipath signals from the original correlation results, which means:

$$R'_k = R'_x(\tau_k) = R_x(\tau_k) - \sum_{i=0}^M \hat{\alpha}_i R(\tau_k - \hat{\tau}_i) e^{j\hat{\phi}_i} = \hat{n}(\tau_k). \tag{15}$$

At the same time, by choosing an appropriate time delay  $\tau_{ref}$ , such as 5 chips, the result of the reference correlator can be made to be the measurement of the noise correlation result  $R_{ref} = n(\tau_{ref})$ . Since environmental noise can basically be regarded as white noise, the value of  $R_{ref}$  is not affected by  $\tau_{ref}$ , and is only related to the intensity of environmental noise. Therefore, with selecting an appropriate window period, the result  $S_{ref} = RMS(R_{ref}(t))$  of calculating the root mean square of  $R_{ref}(t)$  can be used as a measurement standard of environmental noise intensity.

Similarly, the result  $S_k = RMS(R'_k(t))$  for  $R'_k(t)$  can also be used as an estimate of the environmental noise intensity, but this estimate is affected by the MEDLL algorithm. If the number of multipath signals in MEDLL is lower than the actual number,  $S_k$  will be greater than the actual noise intensity and  $S_k$  will be weaker than the actual noise intensity.

Suppose that the MEDLL signal processing structure contains  $N$  correlators, the  $S_k$  of multiple correlators is averaged as:

$$\bar{S} = \frac{\sum_{k=1}^N S_k}{N}. \tag{16}$$

Select  $R_{ref}(t)$  and  $R'_k(t)$  in the recent period, calculate  $S_{ref}$  and  $\bar{S}$ , then adjust the number of multipath signals according to the comparison result. The actual number of multipath signals can be gradually obtained. Set a threshold  $e$ , and the multipath signal number adjustment strategy is shown in Figure 3.

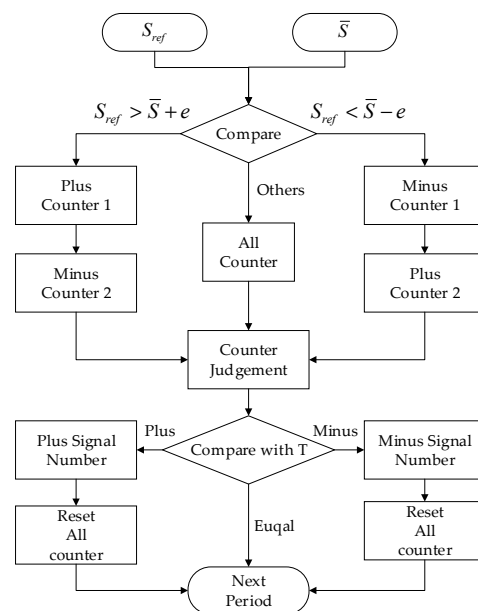
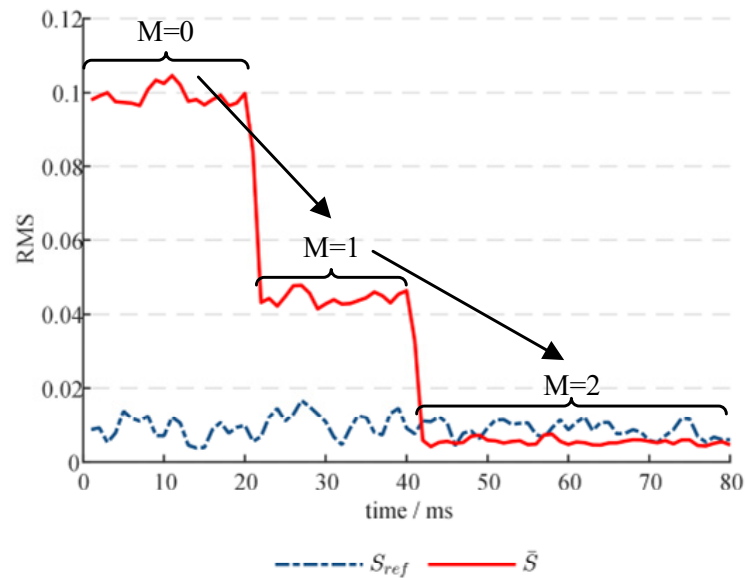


Figure 3. Multipath signal number adjustment strategy.

When the number of multipath signals is 2,  $S_{ref}$  and  $\bar{S}$  change with time as shown in Figure 4. It can be seen that as time passes, the estimated value of the number of multipath signals increases from the initial value 0 to 2 and stabilizes, indicating that the estimation strategy of the number of multipath signals is effective.



**Figure 4.** Multipath signal number estimation process.

However, MEDLL is not good at multipath estimation for short delay multipath signals (less than 0.1 chips). This is due to the fact that the algorithm identifies the short-delay multipath signal and the LOS signal as the same signal. This drawback is easily found in low SNR environments.

However, these multipath estimation errors can be easily monitored. Set the delay threshold  $e_\tau$  and amplitude threshold  $e_\alpha$ , if the condition is satisfied at the same time:

$$\delta\hat{\tau}_i > e_\tau \ \& \ \hat{\alpha}_i < e_\alpha, \quad (17)$$

then the multipath estimation error occurs. The multipath estimation result of this time is discarded, and the result of the last multipath estimation is continued.

## 2.4. Multipath Mitigation Method

### 2.4.1. Method of MEDM

The ultimate purpose of the Ref-MEDLL anti-multipath algorithm is to suppress or mitigate the multipath signals. It can reduce the influence of multipath signals on the subsequent tracking loop of the receiver. Most multipath mitigation techniques based on multipath parameter estimation use the direct elimination method, as follows. It can estimate the number of multipath signals through the previous steps, estimate the parameters of each multipath signal by using the Ref-MEDLL algorithm, and then filter the power of multipath signals one by one through multipath mitigation technology, in order to obtain a direct signal. The influence of multipath effect on pseudolite positioning can be eliminated by iterating the detected multipath signals step by step. After eliminating the detected multipath signals, the correlation curve influenced by gradually peeling multipath signals can be used to replace the original correlation curve for the subsequent calculation curve. The vector tracking loop structure using the direct elimination method is shown in Figure 5.

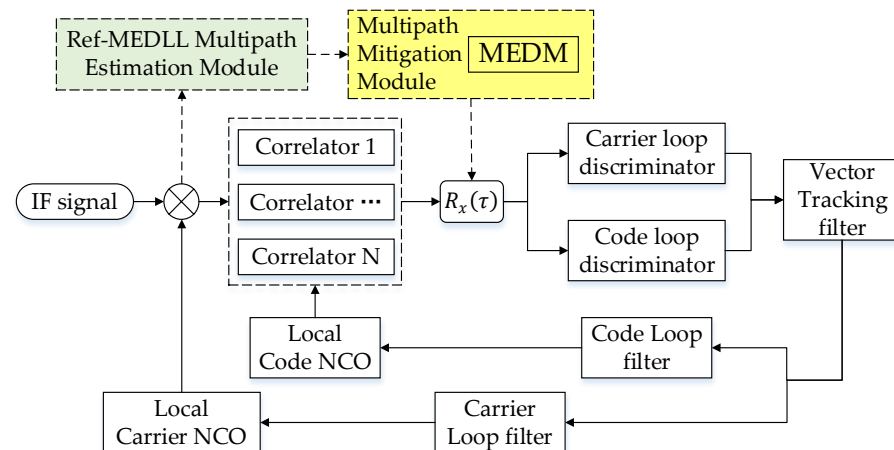


**Figure 5.** Structure diagram of the MEDM method.

Suppose that the original correlation curve is  $R_x(\tau)$ , and the number of multipath estimated by the Ref-MEDLL algorithm is  $M$ , where the amplitude, delay, and phase estimation results of the multipath signal are  $\hat{\alpha}_m$ ,  $\hat{\tau}_m$ , and  $\hat{\phi}_m$ , respectively, then the correlation curve after eliminating the multipath  $R'_x(\tau)$  is

$$R'_x(\tau) = R_x(\tau) - \sum_{m=1}^M \hat{\alpha}_m R(\tau - \hat{\tau}_m) e^{j\hat{\phi}_m} \quad (18)$$

where  $R(\tau)$  is the standard C/A code correlation curve.

After eliminating the multipath signal, the correlation curve after eliminating the multipath is used to replace the original correlation curve for the subsequent calculation, which can mitigate the influence of the multipath effect on the pseudolite positioning.

The direct elimination method works well, but it has to implement one Ref-MEDLL multipath estimation for each pseudolite in each tracking cycle, and the Ref-MEDLL algorithm has high requirements for computational power; therefore, this method requires extremely high computational power in hardware. In order to overcome this problem, this paper proposes the MEAM-VT method to mitigate the influence of multipath effect.

#### 2.4.2. Method of MEAM-VT

In the MEAM-VT method, the Ref-MEDLL multipath estimation module performs multipath parameter estimation at regular intervals.

However, in the Ref-MEDLL algorithm, the computational power to obtain the correlation curve actually is required more to achieve the Ref-MEDLL multipath parameter estimation. When tracking the signal of a pseudolite, only three correlators are required without any multipath rejection algorithm. Multipath suppression algorithms such as the Strobe algorithm require only five correlators. As for the Ref-MEDLL algorithm, when the correlator interval is 0.1 chips, 21 correlators are needed. It can be seen that if the Ref-MEDLL algorithm is applied to pseudolite receivers without any optimization, the receiver is absolutely unable to meet the real-time requirements.

Therefore, in the interval of adjacent Ref-MEDLL multipath parameter estimates, the received signal and the local signal can be stored in the receiver. And a Ref-MEDLL correlator takes turns performing correlation calculations with different delays. It can be assumed that the receiver performs a multipath parameter estimation for 50 milliseconds. During this time, a correlator can perform 41 correlation operations, a correlation curve with a correlation interval of 0.05 code slices can be obtained and the result meets the needs of Ref-MEDLL multipath estimation. At the same time, compared with the original receiver, this algorithm only adds one correlator, and if two correlators are added, similar to multipath suppression algorithms such as the Strobe algorithm, the obtained correlation

curve resolution can even reach 0.025 chips. If the multipath estimation interval is extended, the correlation curve resolution can be further increased. As the time interval for multipath estimation increases, the time limit for each multipath estimation also increases, and the computational power requirements for multipath estimation are greatly reduced. The vector tracking loop structure using the multipath estimation adaptive vector tracking method is shown in Figure 6.

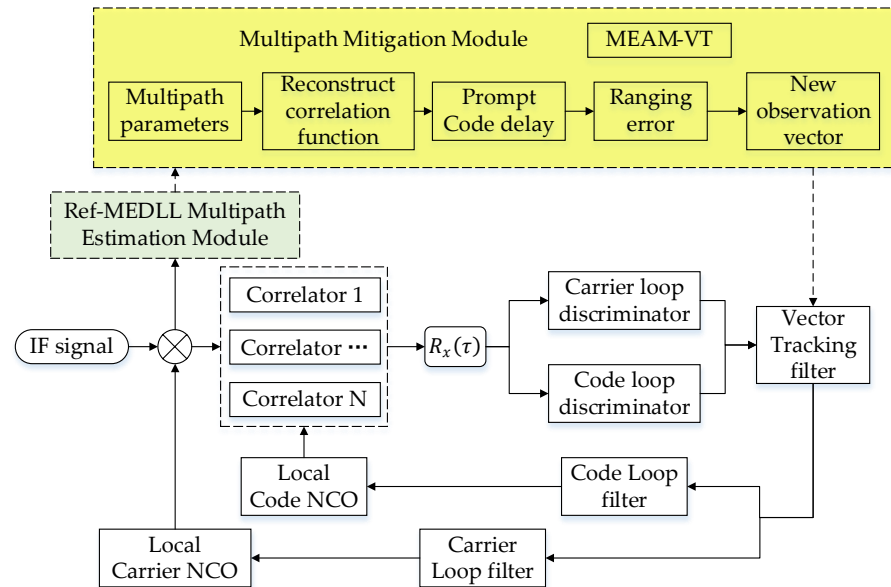


Figure 6. Structure diagram of the MEAM-VT method.

After estimation, the influence of multipath effect on the ranging measurement is calculated according to the multipath parameters, and the observation vector of the vector tracking filter is corrected accordingly. The specific contents are listed as follows:

- Step 1: Multipath parameter estimation based on Ref-MEDLL is performed.
- Step 2: Reconstruction of correlation functions  $\hat{R}_x(\tau)$  can be estimated as:

$$\hat{R}_x(\tau) = \sum_{i=0}^M \hat{\alpha}_i R(\tau_k - \hat{\tau}_i) e^{j\hat{\phi}_i} \tag{19}$$

Step 3: Calculate the value of the prompt code bias caused by the multipath signal, i.e., find a proper value of  $\Delta\tau$  that satisfies Equation (20).

$$\hat{R}_x\left(\tau + \Delta\tau - \frac{1}{2}\delta\right) = \hat{R}_x\left(\tau + \Delta\tau + \frac{1}{2}\delta\right) \tag{20}$$

Step 4: Calculate the ranging error caused by the prompt code bias.

$$\Delta\rho = (\Delta\tau - \tau_0) \frac{c}{f_{code}} \tag{21}$$

where  $c$  is the speed of light;  $f_{code}$  is the C/A code frequency; and  $\tau_0$  is the delay of the direct signal.

Step 5: The multipath ranging error is removed from the observation vector of the vector tracking filter, and then a new observation vector  $Z$  is established, the specific structure of which is shown in Equation (22).

$$Z = [\hat{\rho}_1 - \Delta\rho_1, \dots, \hat{\rho}_N - \Delta\rho_N, \hat{\rho}_1, \dots, \hat{\rho}_N]^T \tag{22}$$

where  $\Delta\rho_n$  represents the ranging error caused by the prompt code bias of the  $n$ th pseudolite.

Finally, the new observation vector  $Z$ , which eliminates the multipath ranging error, replaces the original observation vector and is inputted into the vector tracking filter to eliminate the multipath ranging error.

Compared with the direct elimination method, the multipath estimation adaptive vector tracking method for multipath mitigation greatly reduces the demand for computational power and balances the estimation accuracy and real-time performance to have the best achievement by adjusting the multipath parameter estimation time interval.

### 3. Experiments and Results

Experiments are carried out to verify the performance of anti-multipath vector tracking receiver based on Ref-MEDLL estimator in three aspects: the performance verification of the Ref-MEDLL estimator of the anti-multipath algorithm, and the subsequent positioning impact on the pseudolite receiver. It designs corresponding experiments to test the Ref-MEDLL multipath estimation and mitigation modules, respectively, and analyzes the obtained two modules' parameters. Then, the positioning experiments are implemented on three different receivers, and the positioning results are compared and analyzed.

#### 3.1. Performance of Ref-MEDLL Estimation

The Ref-MEDLL estimation method is mainly divided into two steps: multipath number estimation, and multipath parameter estimation. In this subsection, two experiments are designed to verify the performance of the Ref-MEDLL estimation algorithm. The first experiment is for the use of the Monte Carlo method to test the accuracy of multipath number estimation. The second experiment is for the use of the comparative method to test the performance of multipath parameter estimation.

##### 3.1.1. Multipath Number Estimation

In order to test the performance of the multipath number estimator in the Ref-MEDLL anti-multipath method, a verification experiment of the multipath number accuracy based on the Monte Carlo method is designed. The experiments were carried out on MATLAB simulation platform using GPS L1 PRN1 signal. The ordinary correlator delay is set from  $-1$  chip to 1 chip, with an interval of 0.05 chips, and a total of 41 ordinary correlators. The reference correlator delay is 2 chips.

A total of six group experiments with different multipath numbers were tested from 0 to 9. The multipath signal of each group is generated by a multipath signal generator. In each group, except for the LOS direct signal, each multipath signal is generated by a random method. The signal includes two random numbers, the multipath time delay  $\tau$  parameter variable and the multipath amplitude  $\alpha$  variable. Each set of experiments generates 100 data, and six sets of experiments generate a total of 600 data. After being processed by the Ref-MEDLL multipath number estimator, the accuracy rate of multipath number estimation in each set of data is counted separately. The experimental statistical results are shown in Table 1.

**Table 1.** The accuracy of multipath number estimation results.

Number of Multipath Signals	Accuracy before Correction	Accuracy after Correction
0 (LOS)	100%	100%
1	98%	100%
2	86%	99%
3	71%	91%
4	59%	87%
5	43%	81%
6	26%	42%

From these estimation results in Figure 7, it is concluded that when the number of multipath signals is less than 5, the Ref-MEDLL multipath estimator can basically achieve more than 80% accuracy in estimating the number of multipath signals.

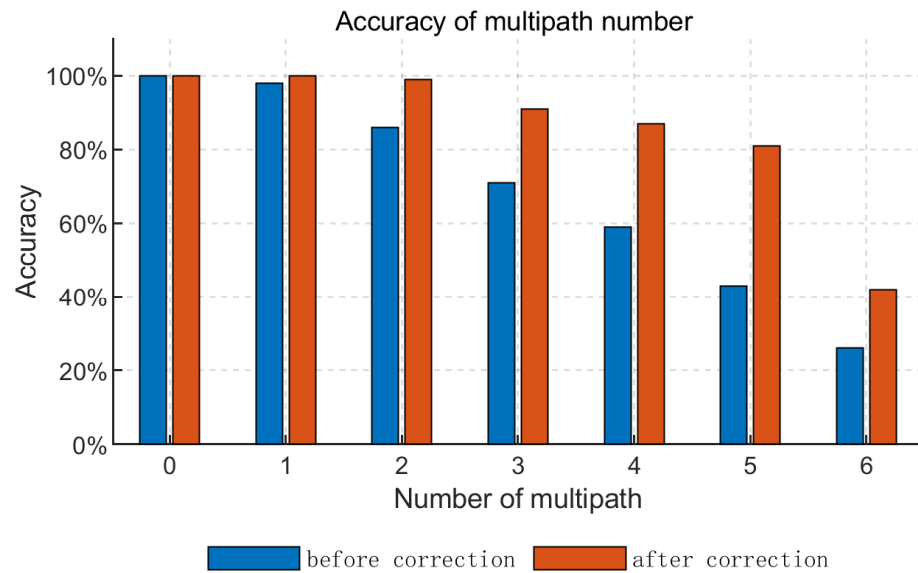


Figure 7. Accuracy of multipath number estimation results.

### 3.1.2. Multipath Signal Parameter Estimation

In order to test the multipath estimation performance of the Ref-MEDLL algorithm under various noise and multipath environments, a comparative experiment is designed for verification. The experiments were carried out on a simulation platform using GPS L1 PRN1 signal. The ordinary correlator delay is set from  $-1$  chip to  $1$  chip, with an interval of  $0.05$  chips, and a total of  $41$  ordinary correlators. The reference correlator delay is  $2$  chips. The MEDLL estimates range from  $0$  chip to  $1$  chip, separated by  $0.05$  chips.

The amplitude of the multipath signal is maintained at  $0.5$  times of the LOS signal, and the time delay is changed. Under different noise environments when the Ref-MEDLL algorithm is applied, the RMSE (root mean square error) of the delay estimation result changes with its actual value, as shown in Figure 8. Lines or dots of the same color in Figure 8a,b represent the same meaning. The  $C/N_0$  of the differently colored curves in Figure 8a is represented by Figure 8b.

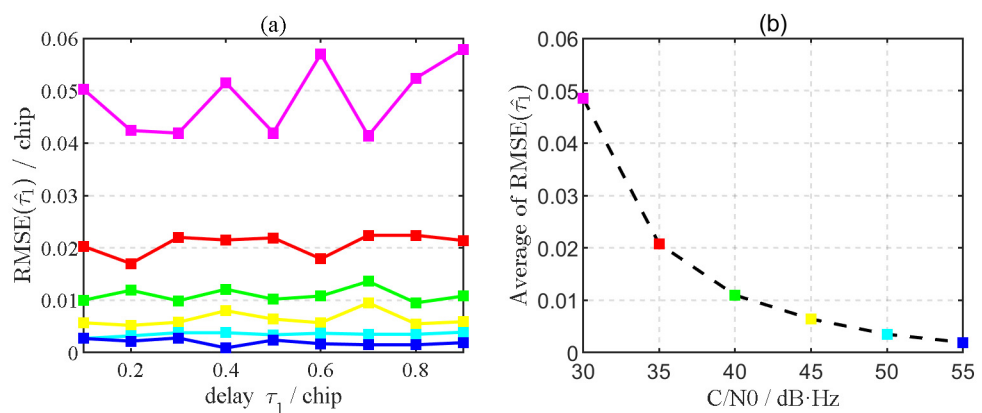
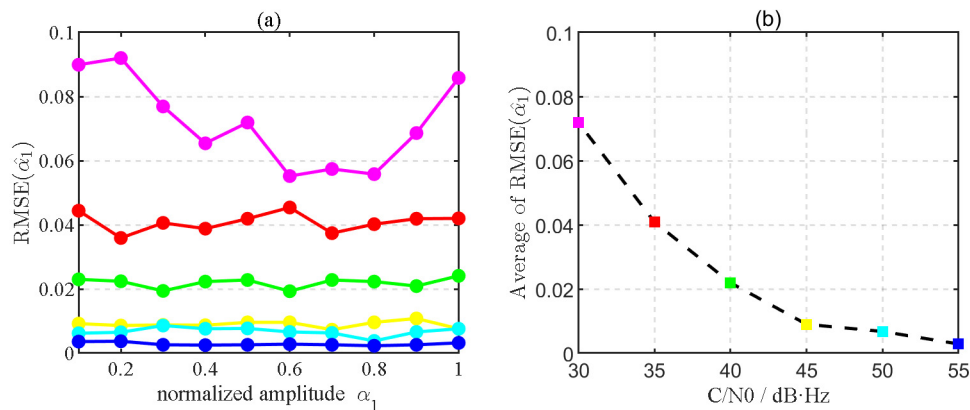


Figure 8. RMSE of delay estimation. (a) RMSE of delay estimation varies with different multipath inputs. (b) The average value of delay RMSE varies with  $C/N_0$  of the input signal.

Similarly, the delay of the multipath signal is maintained at  $0.5$  chips, and the amplitude is changed. Under different noise environments, when the Ref-MEDLL algorithm is

applied, the RMSE of amplitude estimation result changes with its actual value, as shown in Figure 9. Lines or dots of the same color in Figure 9a,b represent the same meaning. The  $C/N_0$  of the differently colored curves in Figure 9a is represented by Figure 9b.



**Figure 9.** RMSE of amplitude estimation. (a) RMSE of amplitude estimation varies with different multipath inputs. (b) The average value of amplitude RMSE varies with  $C/N_0$  of the input signal.

From the experimental results, it can be seen that the Ref-MEDLL has good adaptability to multipath with different amplitudes and delays. Even in low  $C/N_0$  environment, the estimation for multipath signals with different amplitudes and delays does not significantly change with its actual value.

When  $C/N_0$  is 40 dB · Hz, a verification test of Ref-MEDLL multipath signal estimation algorithm is carried out. The test signal is a composite signal simulated by using a GPS signal simulator, including one direct signal DP( $\alpha_0 = 1, \tau_0 = 0$ ) and three multipath signals MP1( $\alpha_1 = 0.6, \tau_1 = 0.5$ ), MP2( $\alpha_2 = 0.5, \tau_2 = 0.8$ ), and MP3( $\alpha_3 = 0.3, \tau_3 = 0.3$ ). The signal is an input to the Ref-MEDLL estimator for multipath signal parameter estimation, and the multipath number estimation step can accurately estimate the above three multipath signals. The detailed parameter results of the estimation are shown in Figure 10. Both direct and multipath signals can be clearly estimated. The higher the amplitude of the multipath signal, the better the parameter accuracy of the estimation.

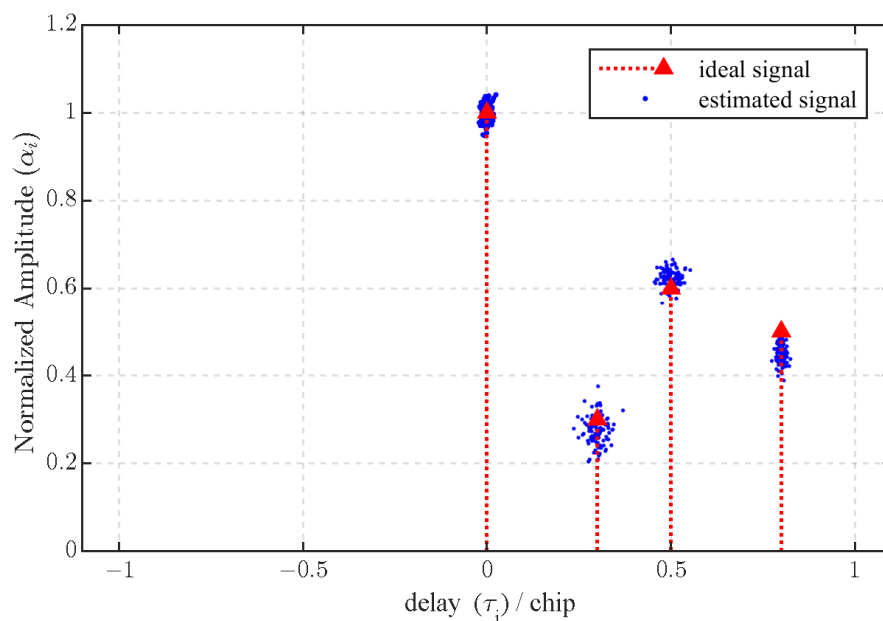


**Figure 10.** The result of multipath signal parameter estimation ( $C/N_0 = 40$  dB · Hz).

As shown in Figure 11, the estimation of the multipath signal obtained by the above experiment highly depends on mean filtering and correlation curve reconstruction to obtain the correlation curves of the direct signal and the three multipath signals. These correlation curves are combined for estimating the correlation curve. By comparing the estimated correlation curve with the actual input composite signal correlation curve, it can be seen that the correlation curve of the estimated signal basically coincides with the correlation curve of the actual input composite signal. This indicates that the accuracy of the estimator can meet the design requirements. The signal parameters of the direct signal and the multipath signal derived by the multipath signal estimator can help in correctly separating the direct signal. This provides the correct parameter input for the subsequent multipath mitigation modules in the receiver.

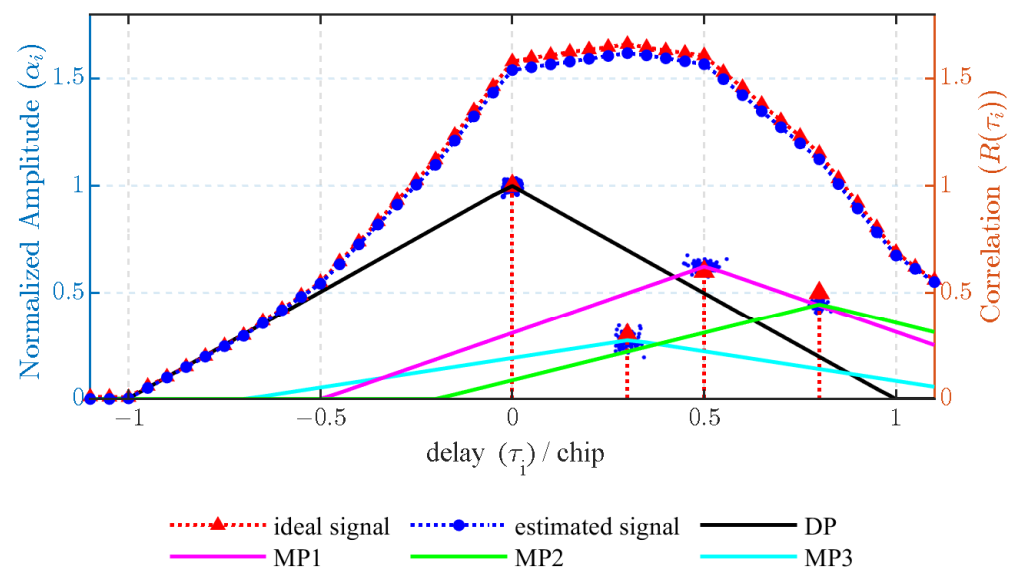


**Figure 11.** The result of multipath signal correlation curve reconstruction ( $C/N_0 = 40 \text{ dB} \cdot \text{Hz}$ ).

### 3.2. Performance of Multipath Mitigation Method

To verify the performance of the proposed adaptive vector tracking receiver multipath mitigation method, this paper designs a comparative experiment for verifying the performance of anti-multipath receiver. It mainly reflects the ability of the receiver to process multipath signals by comparing the tracking results of the tracking loop when processing multipath signals.

The test signals used in this experiment are pseudolite signals and multipath signals generated by the PL signal generator (GNS8440). Its specific parameters are: one direct path (DP) signal, and one multipath signal. The multipath amplitude is equal to 0.5 times the DP signal amplitude, and the multipath delay is equal to 0.5 chips. There are three receivers that were tested in this experiment. The first receiver is a normal receiver without any anti-multipath algorithm, the second receiver is a scalar receiver using the MEDM method, and the third receiver is a new vector tracking receiver using the MEAM-VT method. The experimental results are analyzed at two aspects: multipath mitigation performance and multipath tracking ability, which can reflect the anti-multipath ability of the receiver.

#### 3.2.1. Performance of Receiver Multipath Mitigation

The receiver pseudorange measurement is usually used for positioning, thus it can directly affect the subsequent positioning solution results. Therefore, the anti-multipath performance of the receiver can be obtained directly by comparing the pseudorange measurement of the receiver. The closer the pseudorange value is to the true value, the better its anti-multipath performance.

In Figure 12, “Standard” indicates a normal receiver processing an ideal non-multipath signal; “Normal” indicates a normal receiver processing multipath signal; “MEDM” indicates receiver pseudorange results obtained by the MEDM method; “MEAM-VT” indicates receiver pseudorange results obtained by the MEAM-VT method. It can be seen from Figure 12 that both the MEDM and the MEAM-VT receivers have good multipath mitigation performance compared with the Normal receiver. The pseudorange measurement of the MEAM-VT receiver is closer to the Standard receiver, but its fluctuations are somewhat greater than that of the MEDM receiver.

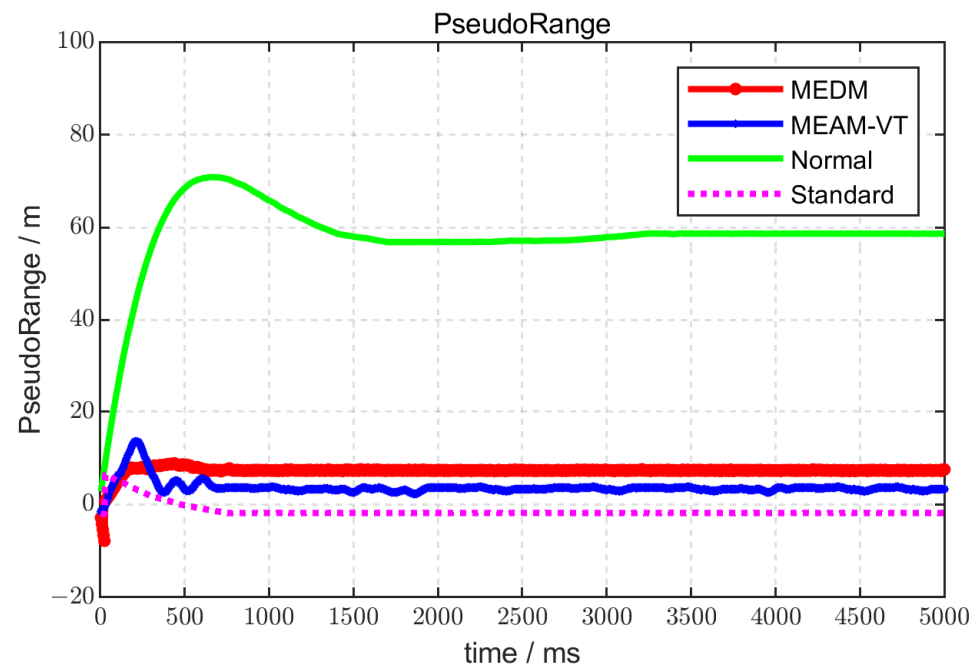


**Figure 12.** The receiver result of the pseudorange measurement.

### 3.2.2. Comparison of the Receiver Tracking Loop Performance

As we all know, the multipath signal will affect the tracking performance of the receiver. Therefore, the tracking performance of the receiver in the steady state can be judged by the code tracking error and the carrier tracking error, which comes from the output of the phase discriminator. Experiments can be designed to compare the tracking loop response results of the above three receivers after processing multipath signals. The result can be used to analyze the receiver tracking results when processing multipath signals. The experiment will analyze the response generated when multipath signals enter the two tracking loops at four aspects, which are the code tracking error from the receiver code tracking loop phase discriminator, the carrier tracking error from the receiver carrier tracking loop phase discriminator, the  $C/N_0$  observation that is used to verify the tracking status of the code, and the unlock detector value that is used to verify the carrier tracking status.

#### (1) Analysis of code tracking error results

In Figure 13, it is shown that the code tracking error is the output of the code tracking loop phase discriminator when three different receivers are processing the same multipath signal. By comparing the data in Figure 13, the code tracking error of the MEDM receiver is the largest, the code tracking error of the MEAM-VT receiver and the Normal receiver is relatively close when processing multipath signals, and the code tracking error of the MEAM-VT receiver does not increase significantly compared with the Normal receiver. Therefore, the analysis results can be obtained: the code tracking loop of the MEAM-VT receiver is stable when processing multipath signals. The MEAM-VT receiver has less noise on the code tracking loop and more stable results compared with the MEDM receiver.

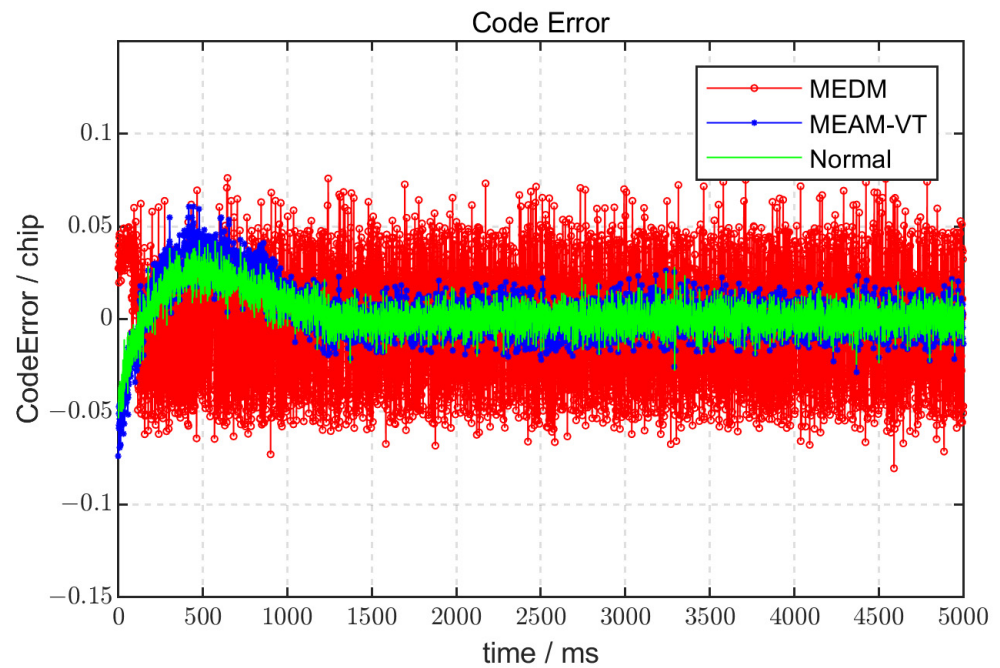


Figure 13. The result of the code tracking error.

(2) Analysis of carrier tracking error results

In Figure 14, it is shown that the carrier phase tracking error is the output of the carrier tracking loop phase discriminator when three different receivers are processing the same multipath signal. By comparing the data in Figure 14, the carrier tracking error of the MEDM receiver, the MEAM-VT receiver, and the Normal receiver is relatively close when processing multipath signals. Therefore, the analysis results can be obtained: the MEDM receiver and the MEAM-VT receiver do not affect the carrier loop tracking results when processing multipath signals.

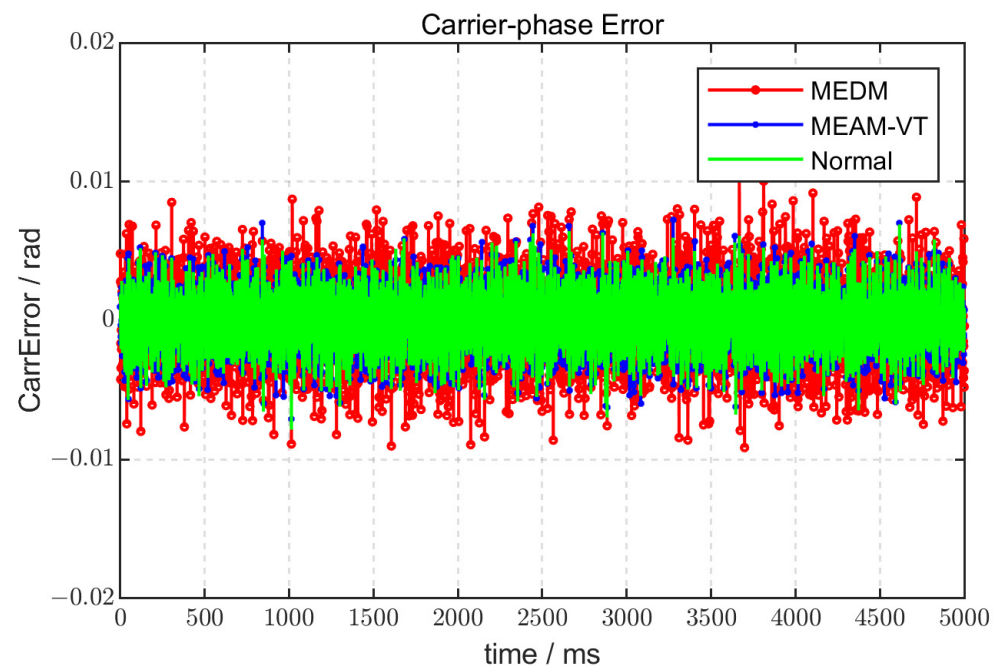


Figure 14. The result of the carrier tracking error.

(3) Analysis of  $C/N_0$  results

The lock detector for the code tracking loop is defined as:

$$\widehat{C/N_0} \underset{\text{lock}}{\overset{\text{no lock}}{\geq}} \gamma_{code} \tag{23}$$

where  $\gamma_{code}$  is the threshold of code tracking loop. If the estimated  $\widehat{C/N_0}$  is above a certain threshold, the tracking loop is declared to be locked. The threshold  $\gamma_{code}$  is set by default to 25 dB·Hz.

In Figure 15, it is shown that  $C/N_0$  is collected from three different receivers when they process the same multipath signal. It can be seen from the change in  $C/N_0$  in the steady state of the receiver that the MEAM-VT receiver and the Normal receiver are basically the same as  $C/N_0$ , and their  $C/N_0$  is significantly higher than that of the MEDM receiver.

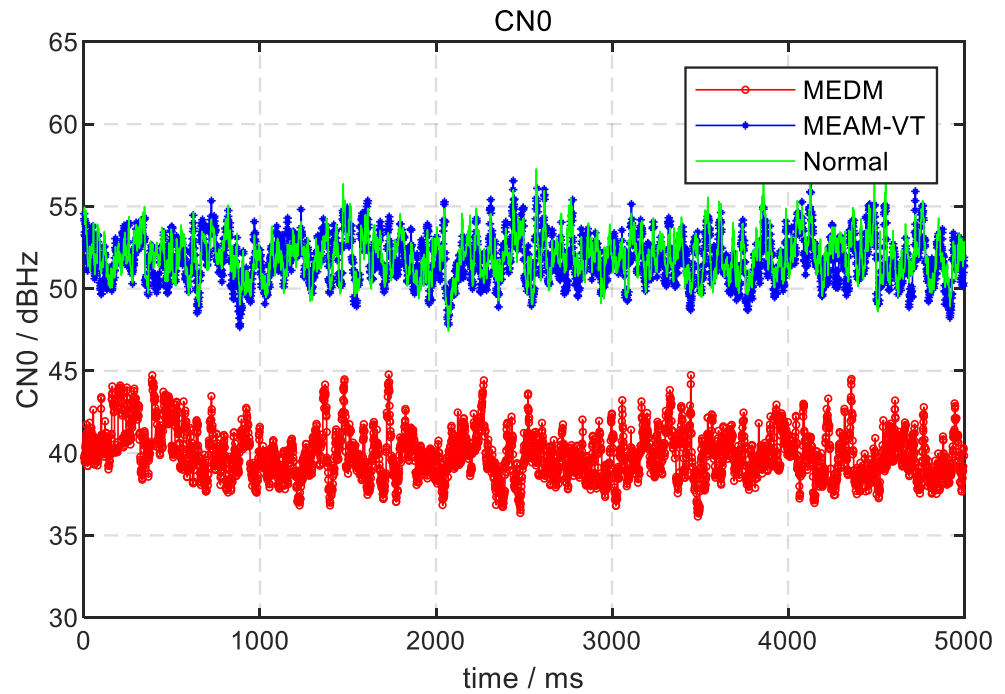


Figure 15. The result of the carrier-to-noise ratio output.

(4) Analysis of carrier lock detector results

The lock detector test for the carrier tracking loop is defined as:

$$LT = \cos(2\widehat{\Delta\phi}) \underset{\text{lock}}{\overset{\text{no lock}}{\geq}} \gamma_{carrier} \tag{24}$$

where  $\Delta\phi = \phi' - \widehat{\phi}$  is the carrier phase error. If the estimate of the cosine is twice the carrier phase error above a certain threshold, the loop is declared to be locked.

In Figure 16, it is shown that LT (lock test) is the output of the carrier tracking detector when three different receivers are processing the same multipath signal. It can be seen from the change in carrier-to-noise ratio in the steady state of the receiver that the MEAM-VT receiver and the Normal receiver are basically the same in LT results, and their carrier-to-noise ratio is significantly higher than that of the MEDM receiver.

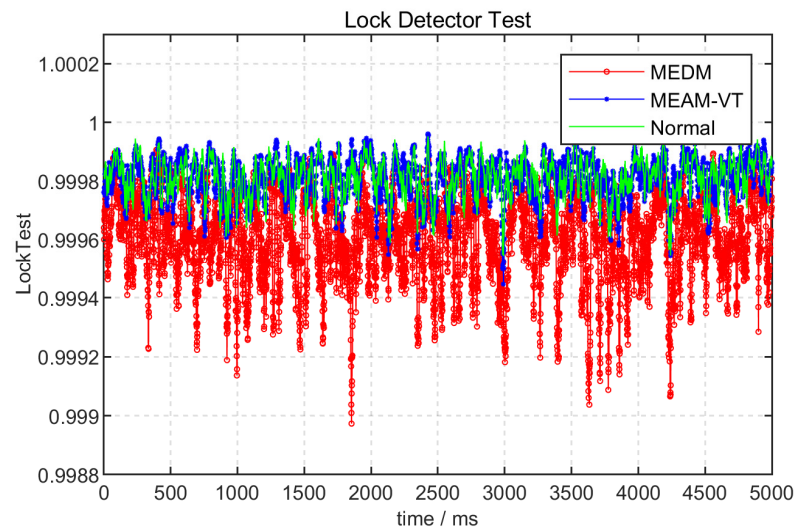


**Figure 16.** The result of the carrier loop.

From the analysis of the above experimental results, it can be concluded that both the MEDM receiver and the MEAM-VT receiver have good multipath mitigation performance, but the performance of the MEAM-VT receiver is better.

After adding the multipath mitigation algorithm, the tracking ability of the MEDM receiver decreased significantly, but the tracking ability of the MEAM-VT receiver and the Normal receiver did not decrease significantly.

In conclusion, both the MEAM-VT method and the MEDM method can be used as multipath mitigation algorithms for anti-multipath receivers, but the MEAM-VT method is superior in tracking performance.

### 3.3. Positioning Experiment and Results

In order to test the effect of multipath mitigation method in practical pseudolite positioning, some experiments are carried out. The pseudolite signal used for indoor positioning is generated by a multi-beam PL signal generator (GNS8460). The experiment environment is shown in Figure 17, with a total of six transmit antennas and one receiver antenna. Two of the transmitting antennas transmit normal satellite signals, and four transmitting antennas transmit multipath signals. The position of the receiver is marked with a red triangle symbol for static experiments, and the forward trajectory of the receiver is marked with a blue arrow symbol for dynamic experiments. Point A and point B are respectively the start and end points of the receiver's trajectory.

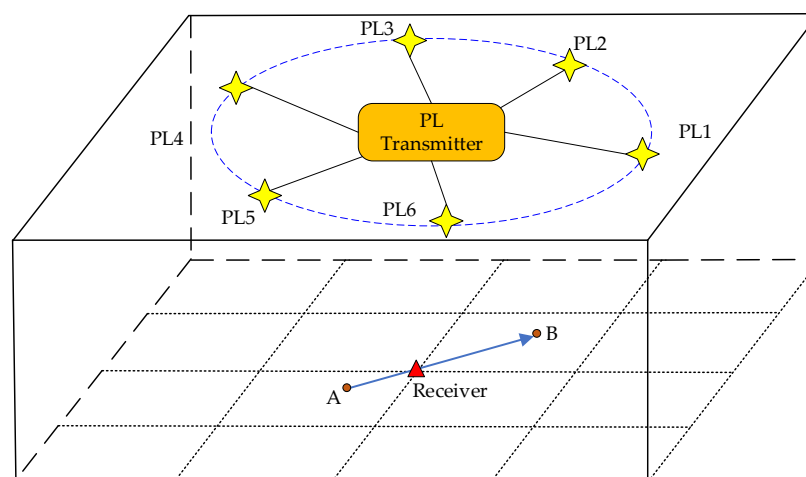


**Figure 17.** The simulation experiment environment.

As for the transmitting antennas, some of their settings are shown in Table 2. The multipath signal amplitude in the table is set to a multiple of the LOS signal amplitude, and the unit of multipath delay is the chip. The simulated signal of PL1 contains two multipath signals, the simulated signal of PL2, PL3, and PL4 contains only one multipath signal, and the PL5 and PL6 do not contain multipath signals. The amplitude and delay settings for each multipath signal are listed in Table 2. All transmitting antennas are approximately distributed on a circle with a radius of 200.

**Table 2.** The setting of the pseudolite transmitting antennas.

Transmit Antennas	Multipath Number	Multipath Signal Setting	
		Amplitude	Delay (Chip)
PL1	2	0.3	0.5
PL2	1	0.3	0.8
PL3	1	0.2	0.6
PL4	1	0.3	0.3
PL5	0	—	—
PL6	0	—	—

As for the receiver, in static experiments, its position is set to (0, 0, 0). In dynamic experiments, the trajectory of the receiver is a straight line passing through (0, 0, 0). The delay of the common correlator was set from  $-1$  chip to  $1$  chip with an interval of  $0.05$  chips, a total of  $41$  common correlators. The delay of the reference correlator is  $2$  chips.

Set the receiver in a static state, and use three algorithms for the received pseudolite signals: no anti-multipath (Normal), multipath estimation direct mitigation (MEDM), and multipath estimation adaptive mitigation of vector tracking (MEAM-VT) for signal tracking and positioning, and use the processing result (Standard) of the ideal non-multipath signal processed by the normal receiver as the true value for comparison. The pseudorange results obtained by the signal transmitted by each pseudolite after being processed by four receivers are shown in Figure 18.

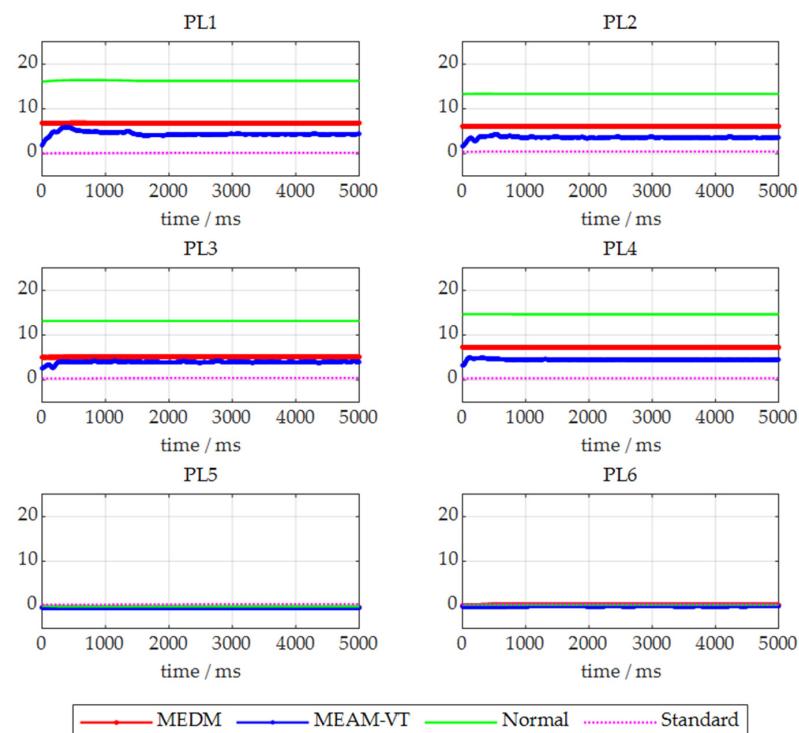


**Figure 18.** The pseudorange result of static positioning experiment.

In static positioning experiment, the pseudorange results vary due to the different multipath parameter settings for each pseudolite and the receiver used to process the signal.

The result of pseudolite positioning is shown in Figure 19. The RMS value of four receivers in static environment are shown in Table 3. The distance between the positioning results of the Normal receiver without the multipath mitigation function and the Standard receiver is the positioning error caused by multipath signal, which is about 13.7 m. The error of positioning result by the MEDM receiver is about 5.9 m; however, the positioning error by the MEAM-VT receiver can be reduced to about 4.2 m. Compared with the Normal receiver, the MEDM receiver has improved the static positioning accuracy by 56.9% and the MEAM-VT receiver has improved the static positioning accuracy by 69.3%. Therefore, it can be seen that both the MEDM receiver and the MEAM-VT receiver have the effect of anti-multipath. The MEAM-VT method has a better anti-multipath effect than the MEDM method.

**Table 3.** The RMS value of four receivers in static environment.

Receiver\Pseudolite	PL1	PL2	PL3	PL4	PL5	PL6
Standard	0.18	0.47	0.40	0.37	0.38	0.42
Normal	15.67	12.97	12.41	14.37	1.50	1.02
MEDM	6.87	6.17	4.61	7.37	1.30	0.82
MEAM-VT	4.72	4.29	4.01	5.25	1.20	0.72

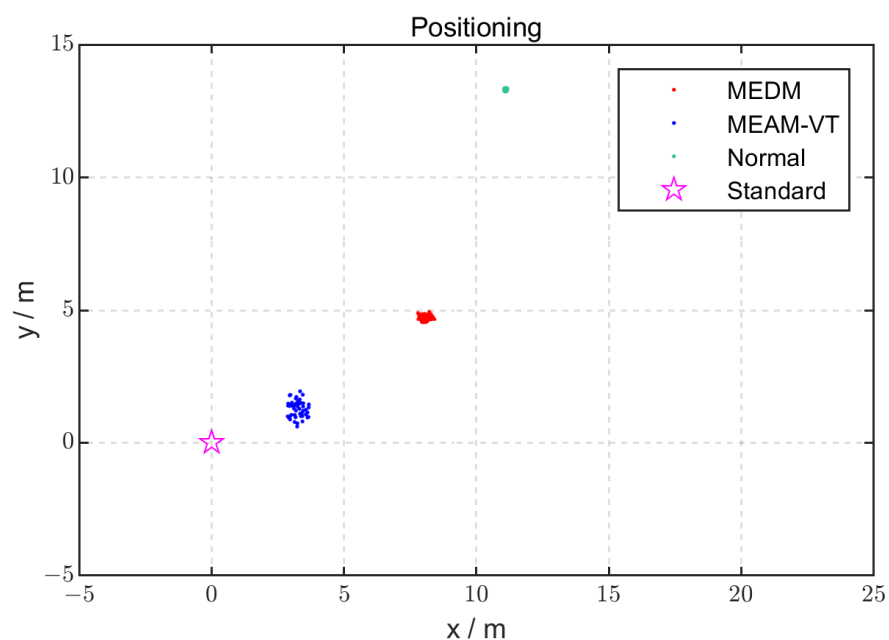


**Figure 19.** The position result of static positioning experiment.

Similar to the static positioning experiment, the actual dynamic positioning experiment is carried out under the environment of  $C/N_0 = 40$  dB · Hz. Set the motion experiment simulation speed to 3.5 m/s, and thus the pseudolite transmitting antenna transmits multipath signals and the settings for multipath signals have not changed. The results obtained by the Normal receiver, the MEDM receiver, and the MEAM-VT receiver are shown in Figure 20. Similar to static results, the distance between the positioning result track of the Normal receiver without multipath mitigation function and the Standard receiver is the positioning error caused by multipath, which is about 114.1 m. The error of positioning result tracked by the MEDM receiver is about 52.2 m; however, the positioning track error by the MEAM-VT receiver can be reduced to about 20.1 m. Compared with the Normal receiver, the MEDM receiver has improved the dynamic positioning accuracy

by 54.3% and the MEAM-VT receiver has improved the dynamic positioning accuracy by 82.4%. Consistent with the conclusions drawn from the static positioning results, both the MEDM method and the MEAM-VT method have the effect of anti-multipath. The MEAM-VT method performs better on anti-multipath than the MEDM method.

The dynamic positioning results obtained by the four different receivers are shown in Figure 20. It can also be seen in Figure 20 that the positioning effect of the MEAM-VT receiver is better than that of the MEDM receiver.

The pseudorange results for the dynamic experiment are shown in Figure 20. The RMS value of four receivers in static environment are shown in Table 4.

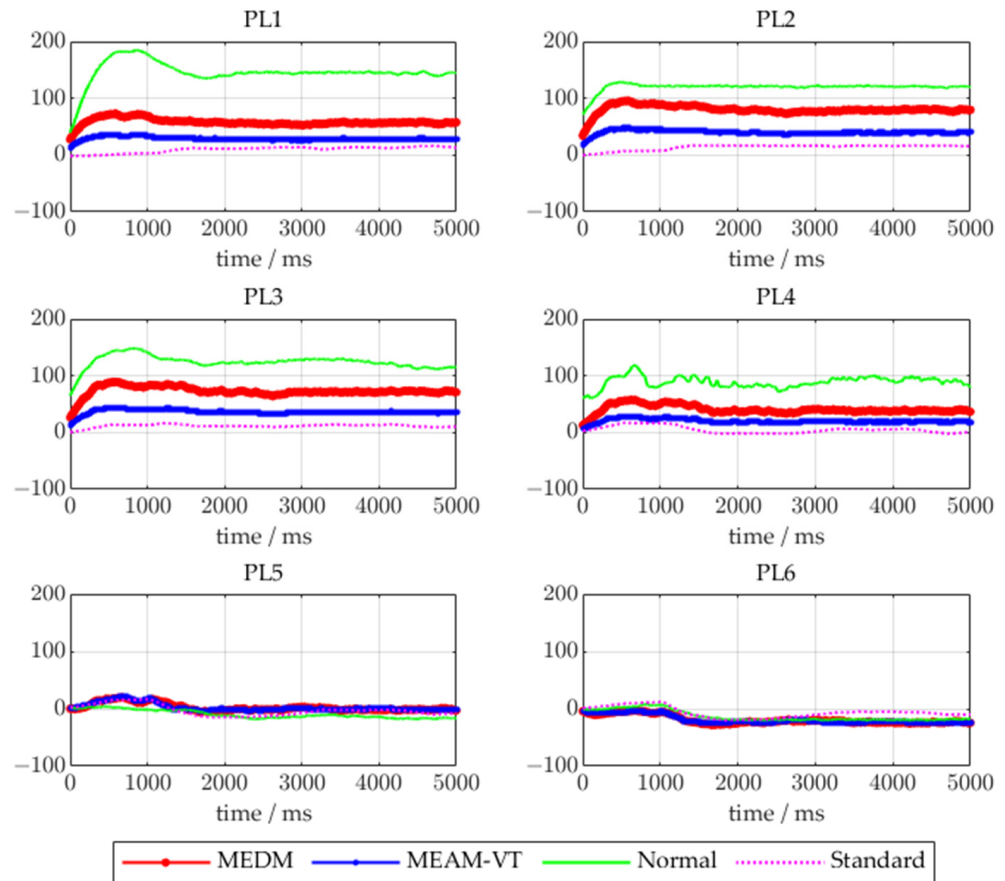


Figure 20. The pseudorange result of dynamic positioning experiment.

In dynamic positioning experiment, the pseudorange results vary due to the different multipath parameter settings for each pseudolite and the receiver used to process the signal.

Table 4. The RMS value of four receivers in dynamic environment.

Receiver\Pseudolite	PL1	PL2	PL3	PL4	PL5	PL6
Standard	11.37	15.03	12.42	8.13	10.21	11.76
Normal	150.67	121.51	127.06	91.07	12.00	16.34
MEDM	59.14	81.79	74.83	42.21	8.27	11.46
MEAM-VT	26.57	43.89	39.41	20.10	7.40	10.94

In summary, the analysis results of the above several experiments show that after using the MEDM and MEAM-VT algorithm in the indoor vector tracking machine, the positioning results have been significantly improved. The positioning results of the four receivers in the dynamic experiment are shown in Figure 21.

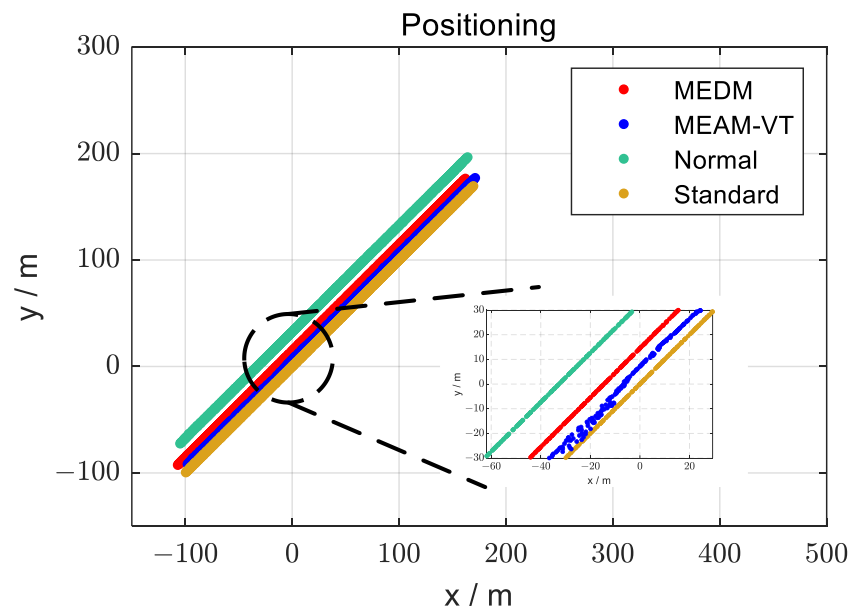


**Figure 21.** The position result of dynamic positioning experiment.

#### 4. Discussion

In this study, two Ref-MEDLL-based multipath signal mitigation methods are proposed, named MEDM and MEAM-VT, respectively. Through the above experiments, it is verified that it has a good impact on the estimation and mitigation of multipath signals. Compared with the traditional MEDLL algorithm, the proposed algorithm adds a reference correlator. The RMS of correlation values of other correlators is taken as the estimate value of noise intensity after all signal correlation curves are eliminated by MEDLL algorithm. Then, the actual number of multipath signals is obtained by the multipath signal number adjustment strategy. Since the algorithm is a measure of noise intensity in essence, it is less sensitive to noise and more suitable for anti-multipath in pseudolite indoor positioning system. Finally, the estimated multipath quantity is substituted into the multipath mitigation module. It uses the elimination method to gradually filter out multipath signals. Therefore, the impact of multipath signals on the subsequent tracking loop of the receiver is reduced.

The following aspects are considered to explore the applicability of the MEDM and the MEAM-VT multipath mitigation method in indoor pseudolite positioning receivers.

##### (1) Noise sensitivity

For multipath signal estimation algorithms, anti-noise performance is the decisive factor to determine the accuracy of multipath parameter estimation. Since the algorithm is a measure of noise intensity in essence, it is less sensitive to noise and more suitable for anti-multipath in pseudolite indoor positioning system.

##### (2) Accuracy of Estimated Results

In the anti-multipath method based on multipath signal parameter estimation, the accuracy of multipath signal and direct signal parameter estimation determines the final positioning accuracy of the anti-multipath receiver [16,35]. The accuracy of multipath estimation is the decisive factor for the receiver to filter out the influence of multipath. The Ref-MEDLL method mainly realizes the estimation of the number of multipath signals by referring to the empirical value of the relevant signal. It adds a rationality judgment verification step of the estimated result of the multipath quantity; therefore, the multipath quantity existing in the received signal can be accurately estimated. The multipath delay parameter estimation method is basically consistent with the traditional MEDLL algorithm; therefore, the reliability of multipath parameter estimation results can be guaranteed.

### (3) Real-time performance [36]

Since the multipath variation of indoor signals is more apparent, the indoor pseudolite receiver puts forward a greater demand for the real-time performance of the multipath suppression algorithm. Compared with other MEDLL and its derivative algorithms, the Ref-MEDLL algorithm only adds the multipath number estimation and judgment methods; therefore, it has little impact on the real-time performance of the overall algorithm. In realizing the anti-multipath receiver based on the Ref-MEDLL method, the operating frequency of the multipath parameter estimation algorithm can be adjusted and controlled to reduce the pressure of the receiver operation. Since the relative motion of the indoor receiver is small, reducing the execution frequency of the multipath estimation algorithm has little effect on the overall anti-multipath effect.

### (4) Comparative Analysis of Indoor and Outdoor Multipath Signal Processing

The influence of indoor environment and outdoor signal on the tracking loop of GNSS pseudolite receiver is different. In an outdoor environment, the altitude angle between the receiver and the satellite changes very slowly; therefore, the multipath environment will not change greatly in a short period of time. On the contrary, in an indoor environment, due to the poor geometric layout of the pseudolite, even if there is a small relative motion between the pseudolite and the receiver, the azimuth and altitude angles of the pseudolite relative to the receiver will change in a short period of time. Large changes will occur, in order that the environment has a significant impact on the short-term changes in the multipath signal. Therefore, compared with outdoor GNSS receivers, indoor pseudolite receivers should improve the update frequency and real-time performance of multipath signal estimation.

### (5) Analysis on the challenges of implementing the Ref-MEDLL + MEDM/MEAM-VT approach in complex environments

Although no single method guarantees perfect accuracy in all situations, the method of this research aims to estimate the multipath signal in the interference to recover the direct signal or cancel the multipath signal. The next work will improve the architecture of the pseudolite receiver to realize the real-time operation of the MEDM and MEAM-VT methods based on Ref-MEDLL, and test them in complex scenarios. In this paper, we demonstrate the feasibility of multipath mitigation in specific scenarios. Subsequently, we will implement enhancements to the receiver to improve the practicality of the anti-multipath method.

In conclusion, while our current research has demonstrated promising results in specific scenarios, we recognize the importance of further refining our methodology and conducting more extensive experiments to validate the effectiveness of the Ref-MEDLL + MEDM/MEAM-VT approach in real-world applications. Although the Ref-MEDLL method has a good influence on multipath number estimation and multipath suppression, this method also has some common problems, such as complex algorithm and relatively large amount of calculation, compared with many multipath estimation methods such as MEDLL. Applications have high demands on the computing power of the processor. In addition, since the actual multipath signals appear in clusters, and the multipath signals are complex and changeable, the number of iterations of this method will increase suddenly. Therefore, subsequent research can simplify the method in this paper and reduce the number of iterations, making it more suitable for real-time receiver.

## 5. Conclusions

In order to solve the problem that pseudolite signals in indoor environment are seriously affected by multipath effect, an anti-multipath receiver using the Ref-MEDLL-based method is proposed in this paper. It adds the Ref-MEDLL multipath estimation module and multipath mitigation module to the traditional receiver architecture. In the multipath mitigation module, the performance of the MEDM and MEAM-VT methods is verified, respectively.

The accuracy of multipath number estimation in the Ref-MEDLL multipath estimation module is tested by the Monte Carlo method. The experimental results show that when the number of multipath signals is less than 5, the Ref-MEDLL multipath estimator can basically achieve more than 80% accuracy in estimating the number of multipath signals. The performance of multipath parameter estimation in the Ref-MEDLL multipath estimation module is demonstrated by the comparative method. The experimental results show that the Ref-MEDLL algorithm has good adaptability to multipath with different amplitudes and delays. Even in low  $C/N_0$  environments, the estimation performance for multipath signals with different amplitudes and delays does not significantly change with its actual value.

This work compares the multipath mitigation performance and tracking loop performance of three receivers, which are the Normal receiver, the MEDM receiver, and the MEAM-VT receiver. The experimental results show that both the MEDM receiver and the MEAM-VT receiver have good multipath mitigation performance, and the multipath mitigation performance of the MEAM-VT method is significantly better than that of the MEDM method. At the same time, the performance of tracking ability is that the MEAM-VT receiver is better than the MEAM receiver. After using the MEAM-VT method in the indoor pseudolite receiver, the positioning results have been significantly improved.

In addition, although the MEAM-VT method of MEAM-VT is highly coupled with the Ref-MEDLL estimator, this multipath mitigation method can not only use the Ref-MEDLL algorithm, but also can use other signal measurement or estimation results. MEAM-VT is based on a vector tracking receiver architecture. As long as the parameters of the multipath signal are taken into the state update equation of the tracking vector, it can affect the tracking loop and achieve the purpose of anti-multipath. In the indoor pseudolite positioning process, the anti-multipath ability of the receiver is particularly important, and the MEAM-VT method can play an important role in the future indoor positioning receiver.

**Author Contributions:** Conceptualization, B.Z. and Q.W.; methodology, B.Z.; software, W.X.; validation, B.Z., W.X. and Q.W.; formal analysis, B.Z. and W.X.; investigation, B.Z.; resources, B.Z.; data curation, B.Z. and W.X.; writing—original draft preparation, B.Z. and W.X.; writing—review and editing, B.Z., Y.S. and J.W.; visualization, B.Z. and W.X.; supervision, Q.W.; project administration, Q.W.; funding acquisition, Q.W. All authors have read and agreed to the published version of the manuscript.

**Funding:** This research was funded by the Jiangsu Provincial Special Fund for Science and Technology (Grant No. BE2022820), the National Key Research and Development Plan of China (grant No. 2020YFD1100202) and the Postgraduate Research & Practice Innovation Program of Jiangsu Province (grant No. KYCX18\_0076).

**Data Availability Statement:** Not applicable.

**Conflicts of Interest:** The authors declare no conflict of interest.

## References

1. Sun, Y.; Wang, J. Mitigation of multipath and NLOS with stochastic modeling for ground-based indoor positioning. *GPS Solut.* **2022**, *26*, 47. [[CrossRef](#)]
2. Gan, X.; Huo, Z.; Sun, L.; Yang, S.; Liu, K. An Approach to Improve the Indoor Positioning Performance of Pseudolite/UWB System with Ambiguity Resolution. *J. Sens.* **2022**, *2022*, 3962014. [[CrossRef](#)]
3. Liu, Q.; Huang, Z.G.; Wang, J.L. Indoor non-line-of-sight and multipath detection using deep learning approach. *GPS Solut.* **2019**, *23*, 75. [[CrossRef](#)]
4. Cheng, L.; Chen, J.; Xie, G. Multipath estimation algorithms based on data processing in software receiver. *Syst. Eng. Electron.* **2013**, *35*, 2050–2056.
5. Lan, C.; Zhiyuan, W.; Jie, C.; Gang, X. An Improved Multipath Estimation Algorithm Using Particle Filter and Sliding Average Extended Kalman Filter. *J. Electron. Inf. Technol.* **2016**, *39*, 709–716. [[CrossRef](#)]
6. Fishler, E.; Bobrovsky, B.Z. Anti multipath cellular radio location for DS/CDMA systems using a novel EKF subchip RAKE tracking loop. In Proceedings of the MILCOM 1999. IEEE Military Communications. Conference Proceedings (Cat. No.99CH36341), Atlantic City, NJ, USA, 31 October–3 November 1999; Volume 1322, pp. 1328–1332. [[CrossRef](#)]

7. Jin Young, K. PN code tracking loop with extended Kalman filter for a direct-sequence spread-spectrum system. In Proceedings of the 30th Annual Conference of IEEE Industrial Electronics Society, 2004. IECON 2004, Busan, Republic of Korea, 2–6 November 2004; Volume 2633, pp. 2637–2640.
8. Lohan, E.S.; Hamila, R.; Lakhzouri, A.; Renfors, M. Highly efficient techniques for mitigating the effects of multipath propagation in DS-CDMA delay estimation. *IEEE Trans. Wirel. Commun.* **2005**, *4*, 149–162. [CrossRef]
9. Wang, X.; Yuan, H. GPS multipath estimation based particle filtering. *Control Decis.* **2010**, *25*, 1139–1143, 1148.
10. Moral, P.D.; Doucet, A. Particle methods: An introduction with applications. *ESAIM Proc.* **2014**, *44*, 1–46. [CrossRef]
11. Zhang, H.Y.; Xu, L.P.; Yan, B.; Zhang, H.; Luo, L.Y. A Carrier Estimation Method Based on MLE and KF for Weak GNSS Signals. *Sensors* **2017**, *17*, 1468. [CrossRef]
12. Yan, S.; Yan, Z. The research on multipath mitigation of GNSS in intelligent crane. In Proceedings of the 2017 IEEE International Conference on Mechatronics and Automation (ICMA), Takamatsu, Japan, 6–9 August 2017; pp. 869–874. [CrossRef]
13. Nee, R.D.J.v. The Multipath Estimating Delay Lock Loop. In Proceedings of the IEEE Second International Symposium on Spread Spectrum Techniques and Applications, Manaus, Brazil, 29 November–2 December 1992; pp. 39–42. [CrossRef]
14. Townsend, B.R.; Fenton, P.C.; Van Dierendonck, K.J.; Van Nee, D.J.R. Performance Evaluation of the Multipath Estimating Delay Lock Loop. *Navigation* **1995**, *42*, 502–514. Available online: <https://onlinelibrary.wiley.com/doi/abs/10.1002/j.2161-4296.1995.tb01903.x> (accessed on 1 January 1995). [CrossRef]
15. Brodin, G.; Daly, P. GNSS code and carrier tracking in the presence of multipath. *Int. J. Satell. Commun.* **1997**, *15*, 25–34. Available online: <https://onlinelibrary.wiley.com/doi/abs/10.1002/%28SICI%291099-1247%28199701%2915%3A1%3C25%3A%3AAID-SAT565%3E3.0.CO%3B2-F> (accessed on 30 October 1996). [CrossRef]
16. Sanchez-Fernandez, M.; Aguilera-Forero, M.; Garcia-Armada, A. Performance analysis and parameter optimization of DLL and MEDLL in fading multipath environments for next generation navigation receivers. *IEEE T Consum. Electr.* **2007**, *53*, 1302–1308. [CrossRef]
17. Tamazin, M.; Noureldin, A.; Korenberg, M.J.; Kamel, A.M. A New High-Resolution GPS Multipath Mitigation Technique Using Fast Orthogonal Search. *J. Navig.* **2016**, *69*, 794–814. Available online: <https://www.cambridge.org/core/article/new-highresolution-gps-multipath-mitigation-technique-using-fast-orthogonal-search/B9A3B467619B2CA9DCA12DD1709A6F25> (accessed on 3 February 2016). [CrossRef]
18. Qin, H.L.; Xue, X.; Yang, Q. GNSS multipath estimation and mitigation based on particle filter. *Let Radar Sonar Nav.* **2019**, *13*, 1588–1596. [CrossRef]
19. Wang, P.; Morton, Y.J. Multipath Estimating Delay Lock Loop for LTE Signal TOA Estimation in Indoor and Urban Environments. *IEEE T Wirel. Commun.* **2020**, *19*, 5518–5530. [CrossRef]
20. Im, S.H.; Jee, G.I. Indoor Navigation and Multipath Mitigation Using Code-Offset Based Pseudolite Transmitter Array. In Proceedings of the 2010 International Technical Meeting of the Institute of Navigation, San Diego, CA, USA, 25–27 January 2010; pp. 259–263.
21. Hui, Y.; Song, M.Z.; Meng, B.; Dang, X.Y. An Efficient Method for GPS Multipath Mitigation Using the Teager-Kaiser-Operator-Based MEDLL. *Radioengineering* **2013**, *22*, 1202–1210.
22. Préaux, Y.; Boudraa, A.-O.; Larkin, K.G. On the positivity of Teager-Kaiser’s energy operator. *Signal Process.* **2022**, *201*, 108702. Available online: <https://www.sciencedirect.com/science/article/pii/S0165168422002419> (accessed on 26 September 2021). [CrossRef]
23. Yang, Q.; Qin, H.; Yuan, H. Multipath analysis of GNSS measured data based on TK-MEDLL. *J. Navig. Position.* **2017**, *5*, 117–124.
24. Ya-huan, L.I.U.; Yu, T.; Guo-tong, L.I. GPS Multipath Estimation Based on Maximum Likelihood Estimation. *J. Chin. Soc. Astronaut.* **2009**, *30*, 1466–1471.
25. Tang, B.; Chen, J.; Yang, L.; Wang, L.; Liu, H. GPS Multipath Estimation Based on Colored Noise Kalman Filtering. *Trans. Beijing Inst. Technol.* **2010**, *30*, 1197–1200.
26. Xia, W.Q.; Wang, Q.; Zhang, B.; Yang, Y. Indoor pseudolite multipath estimation algorithm based on adaptive MEDLL. *J. Syst. Eng. Electron.* **2022**, *45*, 2506–2513. Available online: <https://kns.cnki.net/kcms/detail/11.2422.TN.20221228.0756.001.html> (accessed on 6 July 2022).
27. So, H.; Lee, T.; Jeon, S.; Kim, C.; Kee, C.; Kim, T.; Lee, S. Implementation of a Vector-based Tracking Loop Receiver in a Pseudolite Navigation System. *Sensors* **2010**, *10*, 6324–6346. [CrossRef] [PubMed]
28. Xu, B.; Hsu, L.T. Open-source MATLAB code for GPS vector tracking on a software-defined receiver. *GPS Solut.* **2019**, *23*, 46. [CrossRef]
29. Yang, H.T.; Zhou, B.; Wang, L.X.; Wei, Q.; Ji, F.; Zhang, R. Performance and Evaluation of GNSS Receiver Vector Tracking Loop Based on Adaptive Cascade Filter. *Remote Sens.* **2021**, *13*, 1477. [CrossRef]
30. Xu, B.; Jia, Q.Q.; Hsu, L.T. Vector Tracking Loop-Based GNSS NLOS Detection and Correction: Algorithm Design and Performance Analysis. *Ieee T Instrum. Meas.* **2020**, *69*, 4604–4619. [CrossRef]
31. Zhang, M.; Chen, X. Application of improved MEDLL technique in multipath error estimation. *J. Navig. Position* **2019**, *7*, 96–101.
32. Fernandez-Prades, C.; Arribas, J.; Closas, P.; Aviles, C.; Esteve, L. GNSS-SDR: An Open Source Tool For Researchers and Developers. In Proceedings of the 24th International Technical Meeting of the Satellite Division of the Institute of Navigation (Ion Gns 2011), Portland, OR, USA, 20–23 September 2011; pp. 780–794.

33. Townsend, B.; Fenton, P.; Van Dierendonck, K.; van Nee, R. L1 carrier phase multipath error reduction using MEDLL technology. In Proceedings of the Ion Gps-95—The 8th International Technical Meeting of the Satellite Division of the Institute of Navigation, Pts 1 and 2, Palm Springs, CA, USA, 12–15 September 1995; pp. 1539–1544.
34. Qin, H.L.; Jin, X.Q.; Cong, L.; Yao, J.T. MEDLL-based method of ground-wave and cycle identification for Loran-C signal. Proceedings of 2019 14th Ieee International Conference on Electronic Measurement & Instruments (Icemi), Changsha, China, 1–3 November 2019; pp. 114–123.
35. Gao, Y.; Liu, F.; Long, T. Analysis of Multipath Parameter Estimation Accuracy in MEDLL Algorithm. In *China Satellite Navigation Conference (Csncc) 2013 Proceedings: Beidou/Gnss Navigation Applications, Test & Assessment Technology, User Terminal Technology*; Springer: Berlin/Heidelberg, Germany, 2013; pp. 597–606. [[CrossRef](#)]
36. Shen, N.; Chen, L.; Wang, L.; Lu, X.C.; Tao, T.Y.; Yan, J.; Chen, R.Z. Site-specific real-time GPS multipath mitigation based on coordinate time series window matching. *GPS Solut.* **2020**, *24*, 8210. [[CrossRef](#)]

**Disclaimer/Publisher’s Note:** The statements, opinions and data contained in all publications are solely those of the individual author(s) and contributor(s) and not of MDPI and/or the editor(s). MDPI and/or the editor(s) disclaim responsibility for any injury to people or property resulting from any ideas, methods, instructions or products referred to in the content.